A Thermal Equivalent Circuit to Quantify the Effect of Thermal Paste on Heat Flow Through a PM Machine

M. C. Kulan[1], N. J.Baker[1],

[1]School of Electrical and Electronic Engineering; Newcastle University, Newcastle Upon Tyne, NE1 7RU, UK

Abstract— **This paper describes the thermal modeling approach of a permanent magnet alternator (PMA), developed to investigate the quantitative effect of thermal paste added into the machine end winding region. A thermal lumped parameter network is proposed to investigate the principal heat flow paths for a flange mounted alternator. The thermal model is implemented in Simulink, which allows many different heat paths to be easily combined. Since addition of a thermal paste introduces new axial heat flow by conduction paths between the stator windings and frame, the developed thermal network considers the detailed heat flow paths when thermal paste is present. Experimental results are presented which validate the results.**

Keywords— Permanent Magnet, Thermal Modeling, Thermal Paste

I. INTRODUCTION

Thermal analysis is extremely important as part of the electromagnetic design procedure. There is a strong interaction between the electromagnetic and thermal designs as machine losses (copper, iron and friction) are dependent on the temperature variation and vice versa [1]. Any quantified improvement of thermal performance is hence of value to the machine designer.
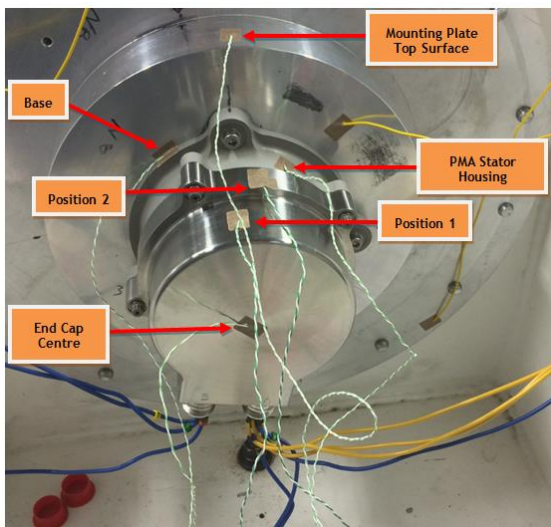

Fig. 1.   Labeled PMA external surfaces

In this paper, the thermal performance of a Permanent Magnet Alternator (PMA), shown in Fig. 1 and detailed in [2], is investigated when joined to the test bed shown in Fig. 2.
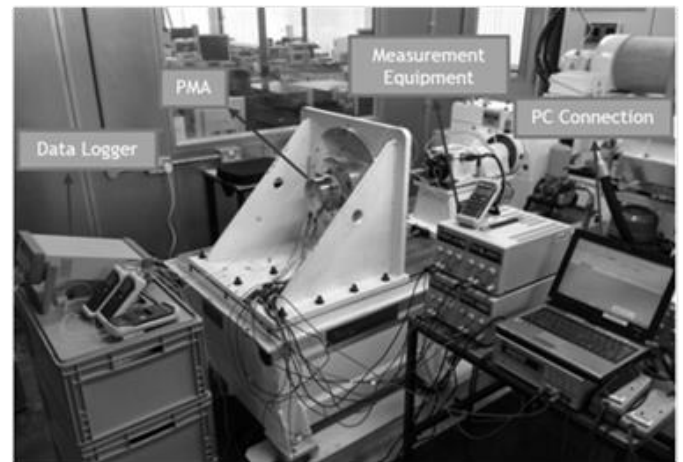

Fig. 2.   Thermal test setup with a large test bench

Although numerical methods such as finite element analysis (FEA) and computational fluid dynamics are very accurate methods to analyze electric machines thermally, e.g. [3], the analytical approach can help designers calculate the temperature variation under certain boundary conditions more quickly [1]. More importantly, they give insight that help designers understand heat transfer mechanisms and main heat flow paths. In this paper it is used as a tool to quantify the thermal advantage of adding a conductive paste to the end windings of the PMA.

In the literature, the majority of reported work on electric machine lumped parameter modeling has addressed traditional induction machines [4]-[6]. The most important aspect of the temperature distribution problem in previous papers is to reduce the hot spot temperature in the machine with a certain distribution of losses [7]-[9]. Thermal investigation is more complicated when a large test bench is considered. Modelling the machine using numerical methods such as transient thermal FEA method might not be achieved without modelling the whole test bench as reaching steady state would take a significant amount of time in the absence of a particular cooling system, leading to a more complicated thermal model.

A convenient lumped parameter thermal modelling approach including radial and axial heat flows has been addressed to investigate thermal performance of the PMA in this paper. The approach is validated experimentally and then used to quantify the effect of thermal paste on heat flow through a PMA.
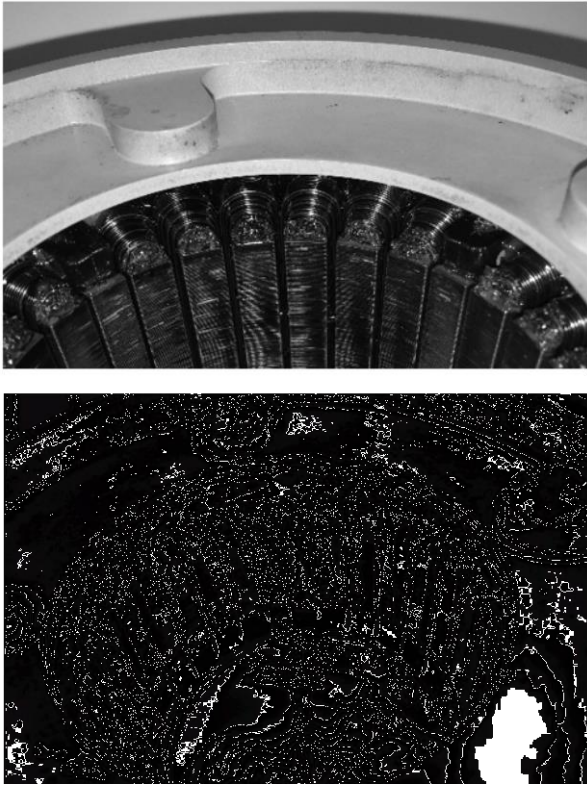

Fig. 3.   Close up of end windings with (right) and without (left) thermal paste

Two identical machines have been tested, where the only difference is that a thermal potting material (Silcotherm AS1420 with 1.38 W/mK thermal conductivity) was added to the end region of the machine to improve the machine cooling, Fig 3. When temperature changes ∆T resulting from injection of a static DC current are compared, it is demonstrated that the prototype with thermal paste gives a better thermal performance. The prototype machine with thermal paste is shown in Fig.4. to have a 14.86% less temperature rise on the external surfaces of the machine and mounting plate. In this paper we present a thermal model to fully investigate the advantage of thermal paste. Adding a new conductive heat path by potting a thermal paste in the end region of the PMA improves the machine thermal characteristic, and the lumped parameter model allows that improvement to be fully quantified.
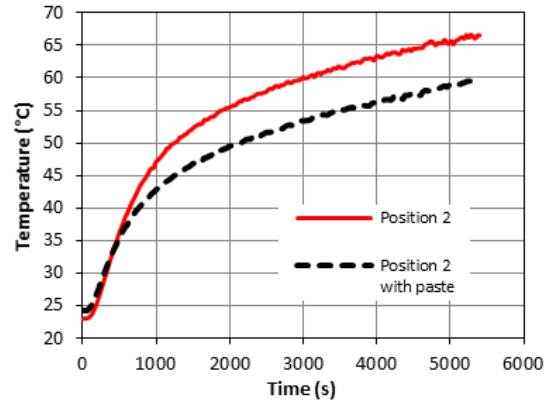

Fig. 4.   Temperature rise with and without thermal paste

II. FEA MODELLING

There are three types external surface in the PMA : vertical plane, horizontal plane and horizontal cylinder for natural convection between the ambient surroundings and the PMA. Since there are no external instruments to cool the machine, only heat transfer by natural convection was considered for the PMA.Heat transfer coefficients for external surfaces, rotor, air gap and end windings were calculated as given in [10]-[11].

There are many physical parameters affecting temperature increase inside the machine such as thermal contact conductance between the PMA and its housing, uncertainty of thermal conductivity for different materials, estimation of heat transfer coefficients for natural convection etc. Therefore, simplification of complex geometry might be useful to manage theoretical and FEA thermal modelling of PMA when it is spinning or stationary. The test rig was illustrated in Fig. 2, and has rough dimensions of 3.15 m × 0.795 m × 0.712 m. This shows how PMA is relatively smaller compared to the test rig - roughly an order of magnitude. In order to reduce thermal modelling complexity for the static thermal tests, the PMA with a mounting plate was isolated from the complete test rig by using 60 mm thick wood pieces under the mounting plate block.

The machine can be further simplified by taking symmetry into account. Therefore, a quarter of the PMA was used in an FEA model to investigate the machine thermal behavior. In this case, the machine cannot be assembled to a full mounting plate due to violated symmetry on the geometry. A time dependent temperature boundary condition was inserted to the top surface of the mounting plate that mimics the thermal behavior of the isolated test rig without distorting the thermal time constant of the proposed model.
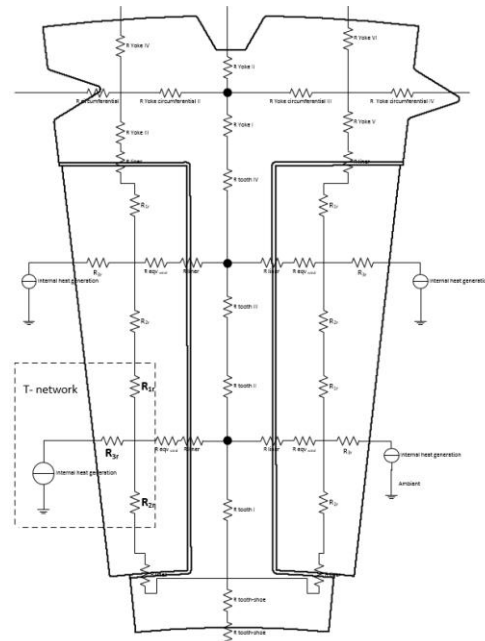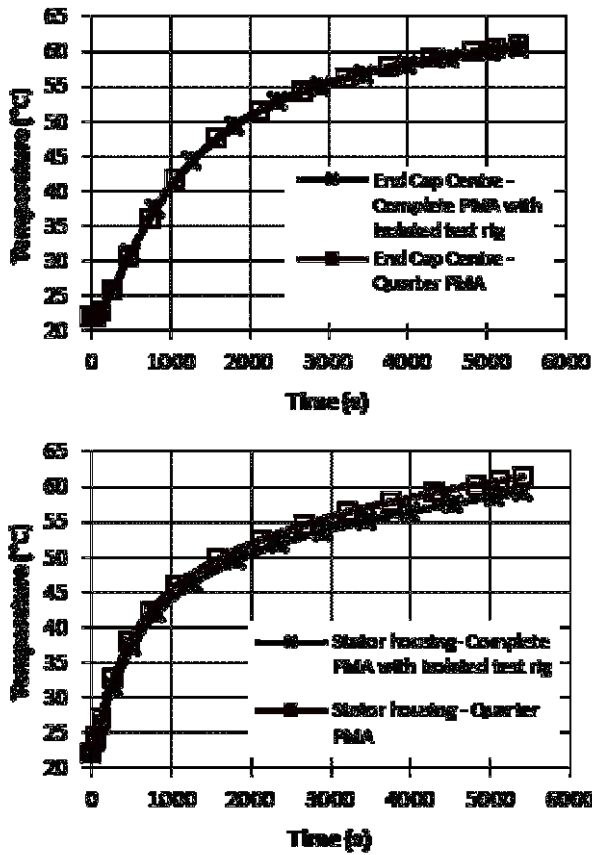
Fig. 5. Comparison of temperature variations for the PMA external surfaces

The models were injected with a DC current to investigate the thermal response. In Fig. 5, temperature variations around the machine casing and stator for full and one quarter FEA models are seen to very close, with less than 5% temperature error. The concept of modelling just one quarter of the machine is hence validated.

III. THERMAL NETWORK

A thermal network was developed to identify the temperatures throughout the PMA including windings, laminations and external casing when only copper losses are injected to the coils at steady state. In much thermal network modelling, authors strive to reduce the number of nodes to simplify computation. Here, the thermal model is implemented in Simulink, which allows many different heat paths to be easily combined. The model incorporates negative compensation thermal resistance, which is represented in Simulink by controlled voltage source (CCVS). It allow us to take full advantage of Simulink software for this application. Thermal network sub-blocks were used for each significant part of the PMA.
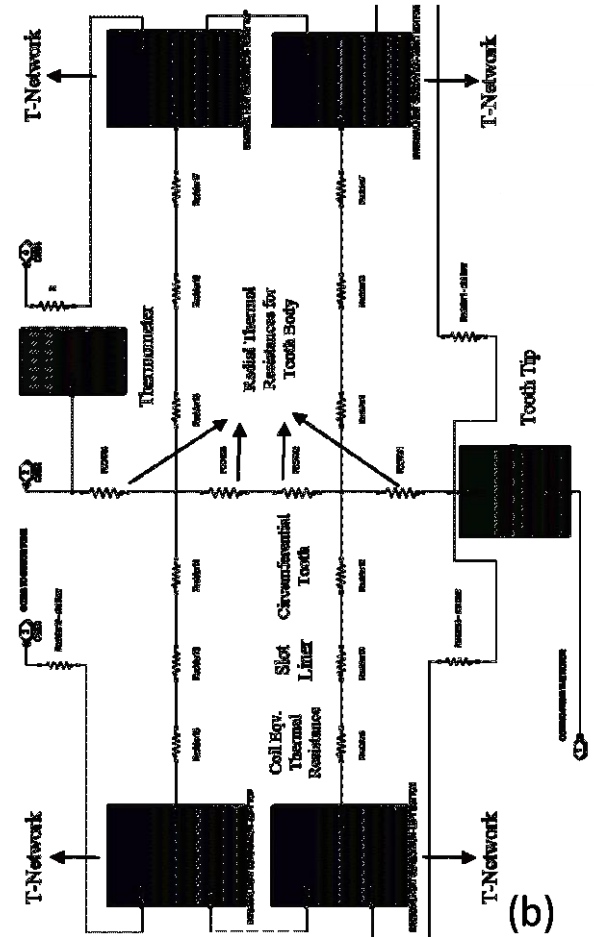
Fig. 6. (a) Tooth – slot equivalent lumped parameter model- only radial (b) Simulink implimnentation tooth-slot sub-block

For determination of thermal resistances, T-equivalent thermal models including radial and axial heat flow wre developed. For example Fig. 6(a) shows the radial heat flow for the PMA tooth-slot geometry.

Since a radial flux machine consists of many heat generating 2D hollow cylinders with inner and outer radius r_1, r_2, thermal conductivity k, and length L, T-equivalent thermal circuit is derived from the heat conduction equations [12]. For radial direction:

$$R_{1r} = \frac{1}{4\pi k_r L}\left[1 - \frac{2r_1{}^2 \ln\left(\frac{r_2}{r_1}\right)}{(r_2{}^2 - r_1{}^2)}\right]$$
(1)

$$R_{2r} = \frac{1}{4\pi k_r L}\left[\frac{2r_2{}^2 \ln\left(\frac{r_2}{r_1}\right)}{(r_2{}^2 - r_1{}^2)} - 1\right]$$
(2)

$$R_{3r} = \frac{-1}{8\pi k_r L(r_2{}^2 - r_1{}^2)}\left[r_2{}^2 + r_1{}^2 - \frac{4r_1{}^2 r_2{}^2 \ln\left(\frac{r_2}{r_1}\right)}{r_2{}^2 - r_1{}^2}\right]$$
(3)

For axial direction:

$$R_{1a} = \frac{L}{2\pi k_a (r_2{}^2 - r_1{}^2)}$$
(4)

$$R_{2a} = \frac{L}{2\pi k_a (r_2{}^2 - r_1{}^2)}$$
(5)

$$R_{3a} = \frac{-L}{6\pi k_a (r_2{}^2 - r_1{}^2)}$$
(6)

Note that R_{3a} and R_{3r} are negative thermal resistances. They are modeled as a current controlled voltage source (CCVS) in Simulink to obtain a negative resistance for thermal modelling of the PMA. For each tooth-slot combination, a thermal sub-model including radial and axial heat flows was created in Simulink. Fig. 6(b) shows the heat flow through the tooth of Fig. 6(a).

IV. THERMAL PARAMETER DETERMINATION

A. Model Implementation

The thermal model was first calibrated to determine important thermal parameters such as thermal conductivity of the winding, frame to stator lamination contact resistance, thermal contact conductance between aluminum stator housing and stainless steel end cap. The calibration is performed by modifying the values within reasonable range

until responses of transient thermal FEA results, thermal lumped parameter model and steady state DC thermal tests match. It is widely accepted that steady state thermal test is mandatory for the determination of the critical thermal parameters [13].

There are some assumptions have been made for thermal modelling of the PMA as follows:

- Heat transfer by radiation was excluded.
- Stator windings were considered to be bulk copper with insulation around and effective thermal conductivity of the slot was predicted by FEA calibration. Effective thermal conductivity of the slot is predicted to be 0.15 W / mK
- Contact pressure which increases thermal contact conductance [14] between the solid bodies was not investigated.
- Since only steady state DC tests were referenced to predict the thermal performance improvement of the PMA with thermal paste, air flow inside the PMA casing and machine airgap was omitted.

Thermal properties of the materials were given in Table I.

TABLE I.   THERMAL PROPERTIES OF THE MATERIALS

Material	Thermal Conductivity (W/mK)	Heat Capacity (kJ kg^{-1} K^{-1})	Density (kg/m³)	Resistivity (Ω m.10^{-8})
Air, stagnant	0.026	1	-	2.7
Aluminum	231	0.899	2700	2.8
Copper	400	0.385	8960	1.75
Magnifier 50 Lamination	13	0.48	8055	-
Stainless Steel	13.8	-	7900	-
Teflon	0.25	1.4	2250	-
Inconel Sleeve	230	0.435	8190	-
Sm Co (PM)	10	0.35	8300	-

In [15], interfacial conductance and interface gap of the metals were tabulated. Thermal contact conductance between stainless steel and aluminum varies between 3000 – 15000 W/m²°C. This is the case when effective gap is in the range 0.0058 – 0.0087 mm. During the thermal calibration process, it was noted that thermal contact conductance between stainless steel end casing and aluminum housing is around 1500 W / m²°C. This implies that there is not a perfect thermal contact between the machine housing parts. However, varying

the thermal contact conductance between the stator housing and end casing in the range: 1000 $W/m^{2o}C$ - 3000 $W/m^{2o}C$ changes the temperature variation on the machine casing in the range 1°C - 3°C as this is not significant temperature difference to cause a substantial temperature distribution error.

Sensitivity analysis was conducted to obtain a thermal contact conductance value between the stator lamination and external stator housing. The interface gap for the PMA, Fig. 7, is relatively large (0.07- 0.09 mm) compared to values given in the literature [1], [16] (0.01 – 0.08 mm), providing poor thermal contact between the stator and machine frame.
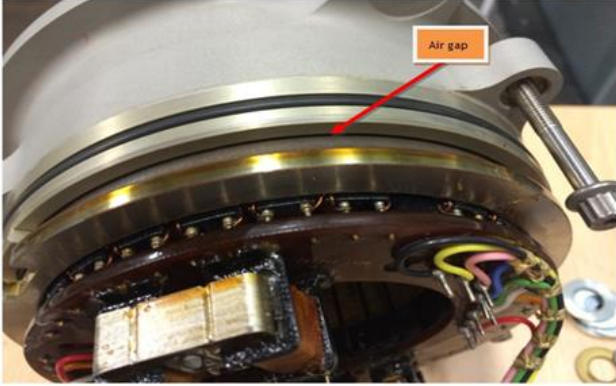

Fig. 7.   1 Airgap between the stator belt and stator housing

By conducting several thermal FEA simulations, the estimated thermal contact conductance is found to be 300 W / m²°C. Fig 8 shows validation by way of a thermal imaging camera and a thermocouple.
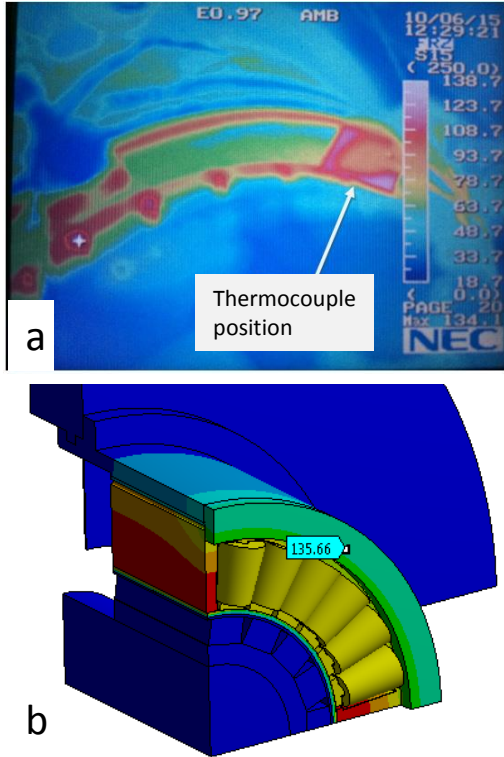

Fig. 8. Determining contact conductance (a) Thermal imaging result in the experiment, (b) FEA thermal result

The obtained thermal contact conductance values are used for the determination of thermal resistances between the contact regions for the lumped parameter modelling. The temperature drop between two contact surfaces is in the form [17]:

$$R_{contact} = \frac{1}{h_{cont} \cdot A} \qquad (7)$$

where, b is called the contact coefficient and A is the surface area of the contact.

B.   Identification of Heat Transfer Coefficients

If a temperature exchange due to the convection exists, the convection resistance is defined as [18]:

$$R_{convection} = \frac{1}{h \cdot A} \qquad (8)$$

where, h (W/m²°C)s the convection heat transfer coefficient for the convection area A. Since thermal modeling is performed for the stationary PMA, speed dependent heat transfer coefficients as proposed in [19]-[20] such as rotor, internal air and end winding convections will not be significant.

The rotor of the PMA was taken as a horizontal cylinder for which temperature dependent heat transfer coefficients are calculated as given in [10]-[11]. The convection heat transfer coefficient between stator winding external connections and inner air can be evaluated as proposed in [11]:

$$h_{ew} = 6.5 + 5.25^{0.6} u_r^{0.6} \qquad (9)$$

As the mounting plate also has a horizontal plate at the bottom, natural convection from a horizontal plate can be predicted using the equations [21]:

$$Nu = \frac{h L}{k} \ , \qquad \text{Pr} = \frac{\mu C_p}{k} \qquad (10 - 11)$$

$$Ra = Gr \ Pr \qquad (12)$$

$$Gr = \left[\frac{L^3 \rho^2 g \Delta T \beta}{\mu^2} \right] \qquad (13)$$

For upper surface:
$$Nu = 0.54 \ Ra^{1/4} \quad (10^4 \leq Ra \leq 10^7)$$
$$Nu = 0.15 \ Ra^{1/3} \quad (10^7 \leq Ra \leq 10^{11})$$

For lower surface:
$$Nu = 0.27 \ Ra^{1/4} \quad (10^5 \leq Ra \leq 10^{10})$$

Dimensionless *Nu*, *Pr* and *Gr* numbers are used to calculate natural heat transfer coefficients. *μ*, *Cp*, *k* denote fluid viscosity (Ns/m²), fluid specific heat (J/g°C)) and fluid thermal conductivity (W/mK) respectively. ρ, g, and β stand for fluid density (kg/m³), gravity and fluid thermal expansion

coefficient (^{0}K^{-1}) respectively. Definition of length parameter is given: L = area of plate / perimeter of plate Correlations of Nu number for upper and lower surfaces are calculated using Ra numbers at given intervals. Heat transfer coefficients were calculated for upper surface: 6.96 W / m^2.^{0}C and for lower surface 1.76 W / m^2.^{0}C when the fluid is stagnant air at ambient temperature (^{0}C).

V. EXPERIMENTAL VALIDATION OF MODELS

In order to demonstrate the accuracy of analytical and FEA thermal models for the prototype machine with thermal paste, a comparison table with relative error between the modelling methods is shown in Table II.

TABLE II.   STEADY STATE TEMPERATURE RESULTS AND RELATIVE ERROR COMPARISON FOR THE PROTOTYPE WITH THERMAL PASTE

Part	Thermal Lumped (°C)	Thermal FEA (°C)	Experiment (°C)	Error (%) FEA -Thermal Lumped	Error (%) Experiment- Thermal Lumped
Shaft	35.74	35.13	36.5	1.706	-2.126
Rotor core back	35.74	35.15	-	1.650	-
Magnets	35.74	35.17	-	1.594	-
Tooth tip	88.92	89.27	-	-0.393	-
Tooth centre	89.07	89.54	-	-0.527	-
Spacer tooth	84.13	81.04	-	3.672	-
Winding	90.05	91.68	-	-1.810	-
Stator core back	78.41	78.22	-	0.242	-
End cap centre	55.03	53.89	56.67	2.071	-2.980
Position 1	61.82	61.85	63.18	-0.048	-2.199
Position 2	55.60	57.03	59.49	-2.571	-6.996
Stator housing	54.89	53.59	52.20	2.368	4.900
Base	46.09	46.30	46.68	-0.455	-1.280

As shown in Table II, relative error between the FEA simulations and lumped parameter model is 3.67%. Also, the error between thermal lumped model and experimental results is 6.99%. Measurements taken from the steady state thermal tests are adequate to quantify the amount of heat flow through the thermal paste by taking axial heat flow into account in thermal lumped model for the PMA with thermal paste.

VI. INVESTIGATING THE EFFECT OF THERMAL PASTE WITH THE THERMAL NETWORK MODEL

Addition of thermal paste to the single side of the stator end region results in axial heat flow becoming a more significant part of the total heat flow inside the machine. In fact, the axial heat flow component is as important as radial the heat component in this case. This is considered in the thermal lumped parameter modeling of the PMA as a new conductive

heat path existing around the stator housing. Therefore, heat flow by conduction occurs for the end windings when thermal paste is added to the PMA end region. Heat flow by conduction for the end windings was modeled in the thermal lumped parameter network. The addition of thermal paste adds additional heat paths from the end winding of the coil to the base of the PMA, Fig.9. For the prototype with thermal paste, since there is no physical contact between the coil end windings, heat transfer by convection occurs between the end windings and internal air. However, when thermal paste is present at the flange side of the prototype, heat transfer by conduction to the machine frame occurs.
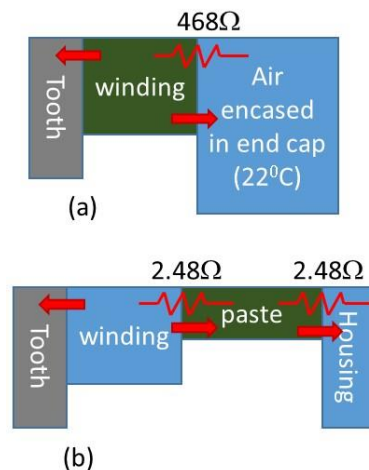

Fig. 9.   (a) Simplified thermal network for the PMA frame; (b) Equivalent thermal circuit representation of axial flow of end winding

The thermal model was validated in Table II. . For a quarter of the PMAs with and without thermal paste, Table III shows heat flowing through significant parts of the PMA when maximum copper loss is injected to the coils.

TABLE III.   MAIN HEAT PATHS AROUND THE PMA WITH THERMAL PASTE

Rate of Heat Flow, watts (joules per second)	PMA with paste	PMA without paste	Unit
Total	49.28	55.3	Watts
Radial	36.88	44.33	Watts
Axial	9.89	7.97	Watts
Rotor heat flow	2.36	3.02	Watts
Heat flow through thermal paste	6.847	-	Watts

As tabulated in Table III, radial heat flow constitutes significant part of the total heat flow (80.16%) for the PMA without thermal paste as axial heat flow occurs only due to heat transfer by convection. Axial heat flow has been improved for the PMA with thermal paste. When 14.4 % of the total generated heat flows axially for the prototype machine with paste, this has been increased to 20% by adding

thermal paste. Therefore, it is clear that average thermal conductivity of the PMA machine has been improved by adding thermal paste since thermal resistance between the end windings and internal air is replaced by lower resistance value: 4.96 °C/W.

VII. CONCLUSION

The main focus of the thermal investigation is to quantify the effect of thermal paste added to the machine end region to improve thermal conductivity between the machine stator and housing. A thermal lumped parameter model for the static case of the PMA has been developed in Simulink, including radial and axial T-Network with thermal compensation resistances. After sensitivity analysis of the PMAs with and without thermal paste, thermal performance of the prototypes have been compared by performing steady state dc tests, FEA simulations and analytical lumped parameter modeling. By performing steady state dc tests, FEA simulations and analytical lumped parameter modeling, it is shown that axial heat flow rate is increased 5.6% for the prototype with added thermal paste.

REFERENCES

[1] A. Boglietti, A. Cavagnino, D. Staton, M. Shanel, M. Mueller and C. Mejuto, "Evolution and Modern Approaches for Thermal Analysis of Electrical Machines," in IEEE Transactions on Industrial Electronics, vol. 56, no. 3, pp. 871-882, March 2009.

[2] N.J. Baker, D. J. Smith, M. C. Kulan, S. Turvey, "Design and performance of a Segmented Stator Permanent Magnet Alternator for Aerospace". In 8th IET International Conference on Power Electronics, Machines and Drives (PEMD 2016), Glasgow, 2016

[3] N. Arbab, W. Wang, C. Lin, J. Hearron and B. Fahimi, "Thermal Modeling and Analysis of a Double-Stator Switched Reluctance Motor," in IEEE Transactions on Energy Conversion, vol. 30, no. 3, pp. 1209-1217, Sept. 2015.

[4] P. H. Mellor, D. Roberts, and D. R. Turner, "Lumped parameter thermal model for electrical machines of TEFC design," Proc. Inst. Elect. Eng. B, vol. 138, no. 5, Sept. 1991.

[5] A. Boglietti, E. Carpaneto, M. Cossale and S. Vaschetto, "Stator-Winding Thermal Models for Short-Time Thermal Transients: Definition and Validation," in IEEE Transactions on Industrial Electronics, vol. 63, no. 5, pp. 2713-2721, May 2016.

[6] A. Boglietti, A. Cavagnino and D. A. Staton, "TEFC induction motors thermal models: a parameter sensitivity analysis," in IEEE Transactions on Industry Applications, vol. 41, no. 3, pp. 756-763, May-June 2005.

[7] M. Galea, C. Gerada, T. Raminosoa and P. Wheeler, "A Thermal Improvement Technique for the Phase Windings of Electrical Machines," in IEEE Transactions on Industry Applications, vol. 48, no. 1, pp. 79-87, Jan.-Feb. 2012.

[8] P. Lindh; I. Petrov; R. Semken; M. Niemela; J. Pyrhonen; L. Aarniovuori; T. Vaimann; A. Kallaste, "Direct Liquid Cooling in Low-Power Electrical Machines - Proof-of-Concept," in IEEE Transactions on Energy Conversion , vol.PP, no.99, pp.1-1

[9] J. D. Widmer, C. M. Spargo, G. J. Atkinson and B. C. Mecrow, "Solar Plane Propulsion Motors With Precompressed Aluminum Stator Windings," in IEEE Transactions on Energy Conversion, vol. 29, no. 3, pp. 681-688, Sept. 2014.

[10] A. Boglietti, A. Cavagnino, M. Lazzari and M. Pastorelli, "A simplified thermal model for variable-speed self-cooled industrial induction motor," in IEEE Transactions on Industry Applications, vol. 39, no. 4, pp. 945-952, July-Aug. 2003

[11] G. D. Demetriades, H. Z. d. l. Parra, E. Andersson and H. Olsson, "A Real-Time Thermal Model of a Permanent-Magnet Synchronous Motor," in IEEE Transactions on Power Electronics, vol. 25, no. 2, pp. 463-474, Feb. 2010.

[12] Lim Chin Hong, "Thermal Modelling of the Ventilation and Cooling inside Axial Flux Permanent Magnet Generators," PhD Thesis, Durham, United Kingdom, 2010.

[13] A. Boglietti, E. Carpaneto, M. Cossale and A. Lucco Borlera, "Stator thermal model for short-time thermal transients," Electrical Machines (ICEM), 2014 International Conference on, Berlin, 2014, pp. 1415-1421.

[14] Lim Chin Hong, "Thermal Modelling of the Ventilation and Cooling inside Axial Flux Permanent Magnet Generators," PhD Thesis, Durham, United Kingdom, 2010.

[15] D. Staton, A. Boglietti and A. Cavagnino, "Solving the More Difficult Aspects of Electric Motor Thermal Analysis in Small and Medium Size Industrial Induction Motors," in IEEE Transactions on Energy Conversion, vol. 20, no. 3, pp. 620-628, Sept. 2005.

[16] W. L. Soong, "Thermal Analysis of Electrical Machines: Lumped-Circuit, FE Analysis and Testing." Tc 2.P3: P4

[17] G. Dajaku and D. Gerling, "An improved lumped parameter thermal model for electrical machines." In 17th International conference on electrical machines (ICEM2006).

[18] Holman J. P., "Heat Transfer", McGraw- Hill Publishing Company, 1990.

[19] G. Kylander, "Thermal modelling of small cage induction motors," Ph.D. dissertation, School Electr. Comput. Eng., Chalmers Univ. Technol., Goteborg, Sweden, Tech. Rep. 265, Feb. 1995.

[20] J. Lindstom, "Thermal model of a permanent-magnet motor for a hybrid electric vehicle," Dept. Power Eng., Chalmers Univ. Technol., Goteborg, Sweden, Internal Rep., Apr. 1999.

[21] F.P. Incropera, D.P. DeWitt, T.L. Bergman, and A.S. Lavine, "Fundamentals of Heat and Mass Transfer", 6th Ed., Hoboken, NJ, John Wiley & Sons, 2007.